Nuclear Considerations for the Application of Lanthanum Telluride in Future Radioisotope Power Systems

Michael B. R. Smith
Oak Ridge National Laboratory (ORNL)
1 Bethel Valley Rd., PO Box 2008 Oak Ridge, TN
865-314-9717
smithmb@ornl.gov

Christopher Whiting
University of Dayton Research Institute (UDRI)
300 College Park, Dayton, OH 45469
937-229-2570
christofer.whiting@udri.udayton.edu

Chad Barklay
University of Dayton Research Institute (UDRI)
300 College Park, Dayton, OH 45469
937-229-3167
chadwick.barklay@udri.udayton.edu

Abstract—**Thermoelectric-based radioisotope power systems (RPSs) produced in the United States convert the heat generated by the radioactive emission of alpha particles from plutonium dioxide ($^{238}PuO_2$) into electricity by means of the Seebeck effect [1]. Certain designs for thermoelectric convertors propose the use of lanthanum telluride (La_3Te_4) materials due to their significant conversion capabilities [2]. The generation of neutrons from spontaneous fission and alpha-neutron (α,n) reactions is also associated with the decay of $^{238}PuO_2$. A portion of these neutrons will interact with the thermoelectric materials and induce trace amounts of transmutation reactions in various lanthanum and tellurium isotopes. While very small quantities of several transmutation products are predicted, the most significant reaction channels are expected to produce trace amounts of iodine which will accumulate over time. Although iodine is classified as a halogen, it is the least reactive of the halogens, and as such, it is the most likely to be able to chemically convert back into the molecule I_2. Since I_2 is a gas at RPS temperatures, it may be possible for iodine to attack other components in the thermoelectric cavity of an RPS system. Iodine reacts easily with metals to produce a wide variety of salts. This behavior could affect the performance of La_3Te_4 thermoelectric devices, particularly the segmented architectures that include multiple sets of bonding and metallization layers. In this type of architecture, several segments of different thermoelectric materials are joined to increase the average thermoelectric figure of merit over a relatively large temperature gradient. It is plausible that sophisticated bonding/metallization layers could be required to join the segment interfaces to each other and to the cold- and hot-shoe materials. The long-term stability and performance of these segmented material combinations could degrade as a result of the potential formation and reactions of metal-iodide compounds at the segment interfaces. This paper (1) investigates the degree to which, if any, this process may threaten potential La_3Te_4 thermoelectric technologies, (2) presents calculations of the amount of iodine generated over the operational life of a radioisotope thermoelectric generator design, and (3) discusses the potential effects of the resulting material's chemical reactions in a segmented couple-level architecture containing La_3Te_4. Conclusions drawn from combined particle transport, transmutation, and thermochemical calculations for La_3Te_4 thermoelectric materials undergoing a notional 20-year mission scenario suggest that there is no significant potential for transmutation-induced thermoelectric (TE) performance degradation.**

TABLE OF CONTENTS

1. INTRODUCTION 1
2. GENERAL COMPONENTS, CONCEPTS, AND CONCERNS FOR THE ADVANCED RTG AND OTHER RPS THERMOELECTRIC MATERIALS 2
3. RADIOACTIVITY AND TRANSMUTATION 3
4. METHODS OF PARTICLE TRANSPORT AND TRANSMUTATION CALCULATIONS 4
5. PARTICLE TRANSPORT AND TRANSMUTATION RESULTS 6
6. CHEMICAL CONSIDERATIONS 7
7. CONCLUSIONS 9
ACKNOWLEDGMENTS 10
REFERENCES 10
BIOGRAPHY 11

1. INTRODUCTION

Radioisotope power systems (RPSs) have a long history of providing electrical power to various spacecraft in the US space industry [3]. While *RPS* is a general term for any system that converts the decay heat (thermal power) of a radioisotope into electrical power, the most common method of power conversion for spaceflight has come from radioisotope thermoelectric generator (RTG) technologies. The process that enables RTG power conversion is a phenomenon known as the Seebeck effect, which occurs when temperature differentials spanning over two dissimilar materials (i.e., a couple) liberate charge carriers that migrate through the medium to generate a voltage bias [3]. Each individual couple can be combined into a larger system, or generator which includes hundreds of couples, thus stepping up the electrical power to ones, tens, or hundreds of watts of electrical power, depending on the thermal loading of the generator design.

The choice of materials to be used in thermoelectric (TE) couples has been a thriving field of research for decades as researchers attempt to increase conversion efficiency while maintaining structural integrity and resistance to various modes of material degradation. The thermal-to-electrical conversion efficiency for a material is frequently discussed using the dimensionless figure of merit *ZT*. Since ZT is dependent on temperature, the efficiency of a TE material can change over a temperature gradient. One proven method for improving the average ZT is to use a couple that contains segments with different TE materials [4]. Each segment can then be selected to operate at high efficiency given the temperature range. These segments must be bonded together to maintain mechanical integrity within an RTG, as the couple's mechanical integrity is necessary to maintain its electrical integrity (i.e., power production).

A design study for the Advanced Radioisotope Thermoelectric Generator (ARTG) proposed the use of lanthanum-telluride (La_3Te_4) TE modules—or modules with La_3Te_4 segments—as a new, innovative approach to increasing thermoelectric efficiency [2]. The elements La and Te have isotopes with potential neutron absorption probabilities (or cross sections) which may facilitate isotopic transition or transmutation into isotopes that present potential negative thermomechanical or chemical performance implications for TE materials.

This investigation used Monte Carlo particle transport techniques to simulate representative materials and neutron fluxes. These simulations were then used to solve transmutation and decay calculations to derive potential isotopic concentrations created over a notional 20-year mission lifetime. The calculated isotopic concentrations were then analyzed using thermochemical software to resolve whether any interaction potentials exist between the transmuted elements and the materials comprising the thermoelectric elements.

2. General Components, Concepts, and Concerns for the Advanced RTG and Other RPS Thermoelectric Materials

Since the Galileo mission in 1989, RPS designs have been based on a PuO_2 fuel form involving iridium fueled clads (FCs) and graphite aeroshell housings known as general purpose heat sources (GPHSs) [5]. The GPHS design is a result of modularizing the heat load and thus the electrical output of a given RPS. The GPHS design also includes an extensive safety program designed to decrease the probability of fuel release in the event of a launch failure or unscheduled atmospheric Earth re-entry scenario [6]. Each GPHS contains four FCs and is designed to stack vertically according to the needs of a given RPS design [Figure 1].

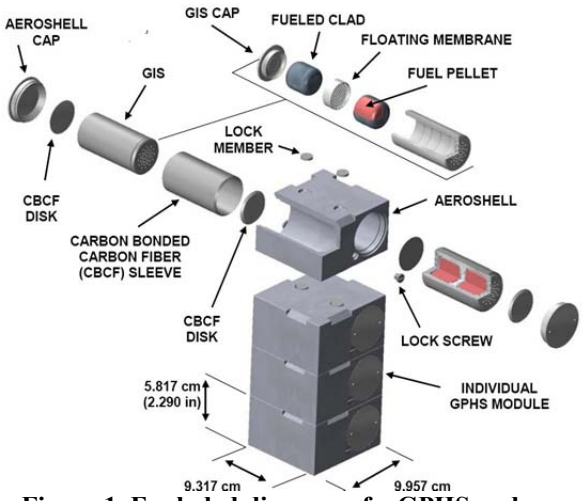

Figure 1. Exploded diagram of a GPHS and an example of traditional vertical stacking

The modularity of the GPHS has been demonstrated in two RPS designs with proven flight heritage: the GPHS-RTG and the Multi-Mission RTG (MMRTG). Table 1 shows high-level comparisons of system performance, design specifications, and mission use of the GPHS-RTG and the MMRTG used currently and historically in spaceflight.

Table 1. General comparison of all historic and current RPS designs using GPHS technology [1, 6].

	GPHS-RTG	MMRTG
GPHS #	18	8
PuO_2 Mass (kg)	~10.8	~4.8
Primary Thermoelectric Material	SiGe/SiMo	TAGS/PbSnTe[§]
Thermal Power at BOL[†] in Vacuum (W)	~4,400	~2,000
Electrical Power at BOL[†] in Vacuum (W)	~300	~110
Missions Used (As of 2018)	Galileo (×1) Ulysses (×1) Cassini (×3) New Horizons (×1)	MSL[£] (×1)

[§]Tellurides of antimony, germanium, and silver (TAGS)
[†]Beginning-of-life (BOL) power output accounting for radioactive decay of the fuel
[£]Mars Science Laboratory (MSL).

The concept of improving system efficiency, longevity, and robustness is always a driving force of RTG and TE research and of new, innovative RPS designs based on the GPHSs currently underway. The advanced RTG (ARTG) is the result of one such effort in which advanced thermoelectric materials were studied, along with a modular design to allow the number of GPHS modules in the RTG to

be tailored to specific mission needs [2]. The study presented segmented thermoelectric technology as an option, which included La_3Te_4, Zintls, and Skutterudite (SKD) materials. Figure 2 shows a simplified concept of an ARTG's TE modules as they orient to a GPHS stack.

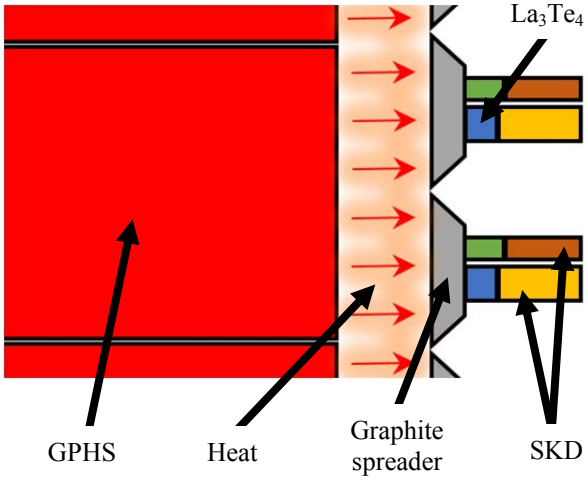

Figure 2. TE Components in a Notional ARTG Design and Orientation to the Vertical GPHS Stack (GPHS, SKD materials, and La_3Te_4 Components Not to Scale)

In general, TE components for RTGs are optimized to generate maximum power for specific nominal operating conditions. However, increased RTG performance can adversely affect system reliability due to degradation mechanisms related to TE material. These mechanisms represent a significant fraction of the overall performance degradation of an RTG over time. Thus, degradation mechanisms must be identified, tested, quantified and modeled to be able to accurately predict the lifetime performance of RTGs. Radiation resistance is a potential degradation mechanism to TE materials that is often overlooked and must be proven through testing and modeling. This investigation was targeted at (1) determining any existing neutron-induced chemical production possibilities for La_3Te_4-based TE materials that may cause unanticipated performance degradation, and (2) demonstrating the analytical capability to perform such calculations for any TE material proposed for use in an RPS.

3. RADIOACTIVITY AND TRANSMUTATION

Radioactivity

Radioactive decay is a phenomenon observed in unstable or excited atoms in which particles are emitted from a source-atom until a stable nuclear or atomic configuration is reached. While there are multiple mechanisms of particle emission, this paper only discusses alpha (α) decay and neutron (n) emission as they relate to PuO_2 fuel for RPSs. Some fundamental differences between these two emission types are (1) the α particles are relatively large, (2) the charged particles consist of two protons and two neutrons, which is synonymous to a completely ionized helium nucleus, while (3) neutron emission simply consists of neutrally charged neutrons [8].

The relatively large charge state of an α particle (2^+) indicates that it is significantly influenced by the electromagnetic or Coulombic forces of other nearby atoms. These charge interactions act to continuously slow down a charged particle as it transits through the combined Coulombic field of a bulk material's atoms. The primary decay mode observed in the PuO_2 fuel is α emission from the ^{238}Pu. The typical α energy emitted from ^{238}Pu is ~5 MeV, which is completely attenuated within millimeters of the surrounding fuel meat and cladding materials. While α particles are the main contributor to heat generation in an RPS, their inability to significantly penetrate any solid materials indicates that they are not a consideration for external radiation or transmutation concerns [8].

In addition to the α emission observed from the PuO_2 fuel, ^{238}Pu and other lower abundance plutonium isotopes (e.g., ^{242}Pu, ^{241}Pu, ^{240}Pu, ^{239}Pu, and ^{236}Pu) all contribute to neutron emission. One prevalent source of neutron emission is through the spontaneous fission (SF) of various plutonium isotopes [9]. Other neutron production channels include (α,n) reactions in which α particles interact with certain low-Z (i.e., low atomic number) elements in the fuel, the most notable of which is the (α,n) with naturally occurring ^{18}O. This additional neutron emission represents a significant portion of the total neutron flux from PuO_2 fuel [10]. Figure 3 shows an example of a typical fuel's total neutron emission spectrum with individual contributions from (α,n) and SF. The mean energy of the total neutron spectrum is approximately 2 MeV, which qualifies this as a fast spectrum. The relative energy of a neutron spectrum governs the probability of certain neutron reactions and is important when estimating potential reaction probabilities from a given neutron radiation field.

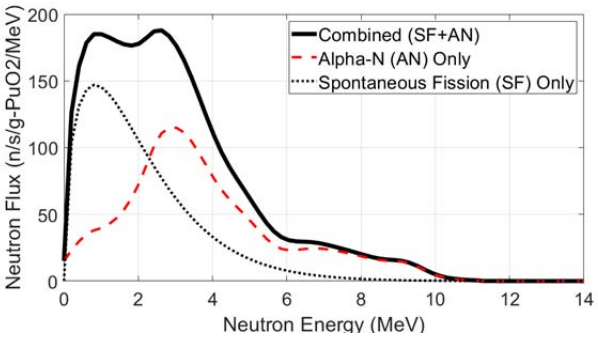

Figure 3. Example of total (solid black), α-n (dashed red), and SF (dotted black) neutron spectra from typical PuO_2 fuel for RPS

Isotopic Transmutation

Free neutrons have a number of reaction possibilities when interacting with other atoms. Reactions can vary from high-energy reactions like spallation to low-energy reactions like fission. Each reaction type is a stochastic process described by a probability distribution quantified as a cross section,

and each reaction-type is typically presented in units of barns (1 barn = 1E-24 cm²). A common transmutation process is when a target atom absorbs a free neutron, the target atom becomes a new isotope, the new isotope β-decays (during which, among other particle emissions, a neutron is converted to a proton), and the new isotope becomes a new element [8]. One of the most significant neutron absorption reactions that contributes to transmutation is the *neutron-gamma* (n,γ) reaction. Figure 4 shows a generic example of a (n,γ) transmutation channel for ^{130}Te, in which it (1) absorbs a free neutron (2), a new isotope (^{131}Te) is produced, and (3) the new isotope β-decays to ^{131}I (3) [11].

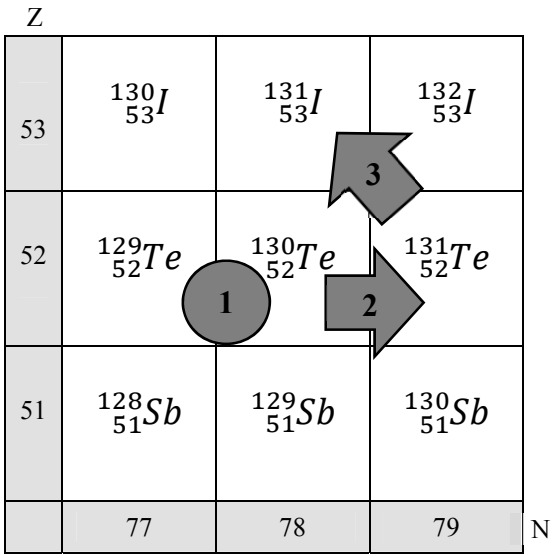

Figure 4. Example of transmutation process in which incident neutron absorption by ^{130}Te (1), produces a radioactive isotope ^{131}Te (2), that subsequently β-decays to ^{131}I (3).

4. Methods of Particle Transport and Transmutation Calculations

Scenarios concerning RPS materials, PuO_2, radiation, and transmutation can be simulated to estimate radiation-induced phenomena using various sophisticated nuclear modeling software packages. This analysis used Monte Carlo N-Particle 6 (MCNP6) for particle transport calculations [12]. Once particle fluxes were calculated for a given scenario, the results were entered into the ORIGEN module of the SCALE software package. ORIGEN uses flux and cross section data to calculate time-dependent isotope concentrations accounting for the decay of unstable isotopes, along with production (or transmutation) of new isotopes due to neutron irradiation [13].

MCNP Simulation Description

MCNP6 allows the user to define geometries, materials, source-particle species, energy spectra, various physics models, and reaction databases for a variety of simulation applications. As a means to asses a worst-case scenario, this particular analysis simulated a notional 18-GPHS configuration with a representative ARTG TE module located at the centerline of the vertical GPHS stack. Figure 5 shows the ray-tracing of a sample set of neutron emissions (A) as they escape the GPHS stack (B), penetrate the TE heat-collector (C), and enter a TE couple (D).

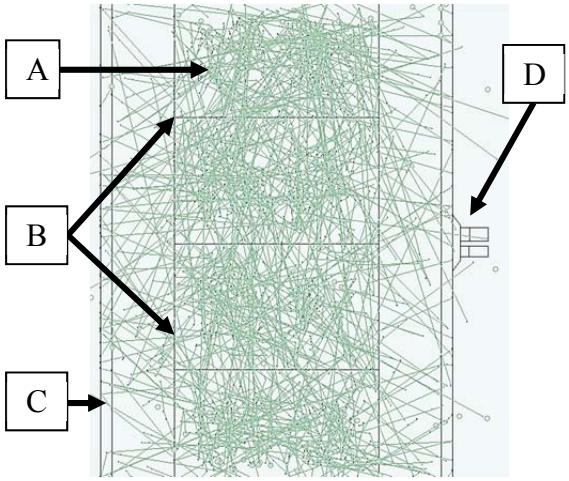

Figure 5. MCNP6 Geometry with Neutron Ray Traces (A), a GPHS Stack (B), a TE Heat Collector (C), and a TE Couple Phantom (D).

Each of the rays in Figure 5 represents a series of stochastically-determined particle paths, or random walks, for a neutron. As each neutron travels from the source region to a TE, it may experience numerous interactions, each of which will either remove the neutron through any number of absorptive reactions or degrade its energy through various scattering mechanisms. Therefore, within any tallied TE module, both the total neutron flux $\left(\frac{n}{cm^2 s}\right)$ and energy spectrum will be different from that in any other region of the problem. Each interaction that a neutron undergoes from birth, through its eventual removal from the system is governed by a continuous-energy description of the cross- section data for any interaction. As an example of continuous-energy interaction probabilities, Figure 6 presents the total neutron cross section for ^{130}Te.

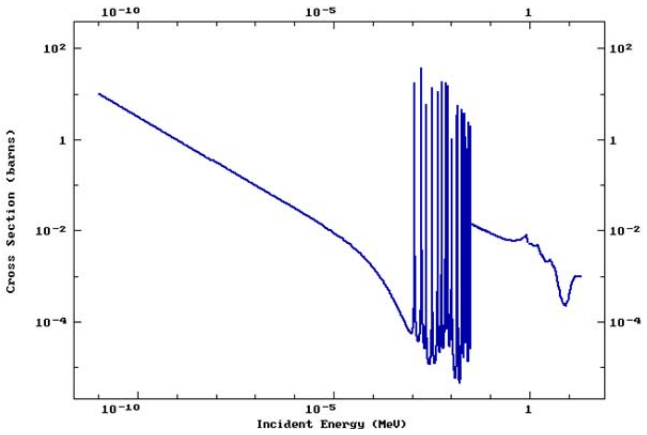

Figure 6. Total Cross Sections for ^{130}Te.

As particles pass through a given geometric cell (e.g., a specific TE), MCNP6 can tally various parameters of interest, including flux and the rates at which specific reactions of interest occur. While the individual particle tracks contribute to the cell average tallies based on the continuous-energy cross section data, the tallies are binned into a finite number of user-defined energy groups to obtain statistically meaningful tallies from a finite number of source particles.

The general expression for nuclear reaction rates is shown in Equation 1, where R_x is the reaction rate $\left(\frac{\text{reactions}}{\text{cm}^3\cdot\text{sec}}\right)$ for reaction *x*, Φ $(\frac{atoms}{cm^2\ sec})$ is the volumetric cell flux, and $\Sigma_x\ (cm^{-1})$ is the effective self-shielded macroscopic cross section for reaction *x* [13]. The macroscopic cross section can further be described as the microscopic cross section $(\sigma_x = cm^2)$ for reaction *x* and the specific isotope *i* multiplied by the atomic number density $(N_A = \frac{atoms}{cm^3})$ for isotope *i*.

$$R_x = \Sigma_x \Phi \rightarrow \Sigma_x = \frac{R_x}{\Phi} = \sigma_x N_A \qquad (1)$$

Note that MCNP6 will tally a separate value of R_x for each isotope in each geometric cell for each energy bin. The use of any subscript notation to delineate these qualifiers has been suppressed for clarity in Equation 1. Using the total reaction rate values (R_x) and volumetric fluxes (Φ) in MCNP6, a one-group (vs. 238-group), self-shielded (vs. infinite-dilute) reaction cross section (Σ_a) for each La and Te isotope is derived for a TE at the mid-plane of the GPHS stack.

SCALE/ORIGEN Calculation Description

The ORIGEN sequence within the SCALE software suite is used to calculate radioactive decay, activation, transmutation, and burnup scenarios using various permutations of the Bateman equation [14]. The expression used in ORIGEN for solving the production and decay of various isotopes is shown in Eq. (2) [13]:

$$\frac{dN_i}{dt} = \sum_{j\neq i}\left(l_{ij}\lambda_i + f_{ij}\sigma_j\phi\right)N_j(t) - \left(\lambda_i + \sigma_i\phi\right)N_i(t) + S_i(t), \qquad (2)$$

where

$\boldsymbol{N_i}$= amount of nuclide i (atoms),

$\boldsymbol{\lambda_i}$= decay constant of nuclide i (#/s),

$\boldsymbol{l_{ij}}$= fractional yield of nuclide i from decay of nuclide j,

$\boldsymbol{\sigma_i}$= spectrum-averaged removal cross section for nuclide i (barns),

$\boldsymbol{f_{ij}}$= fractional yield of nuclide i from neutron-induced removal of nuclide j,

$\boldsymbol{\phi}$ = angle- and energy-integrated time-dependent neutron flux (n/cm²/s), and

$\boldsymbol{S_i}$= time-dependent source/feed term (atom/s).

The flux and cross section values used in ORIGEN's implementation of Equation 2 are one-group values that ORIGEN generates by performing a flux-weighted collapse of the infinite-dilute reaction cross sections contained in the built-in multi-group cross section libraries. These multi-group libraries are derived from point-wise data similar to what was depicted in Figure 6 but collapsed to a large (typically several dozen, to a few hundred) number of groups with a generic flux spectrum. The collapsing from the multi-group cross section values to a one-group value is performed with the cell-specific flux tallied in MCNP6. The flux spectra from MCNP6 is binned into a specific 238-group representation to be consistent with a specific group structure of one of the ORIGEN cross section libraries. Use of the problem-specific 238-group fluxes to collapse the ORIGEN multi-group, infinite dilute cross sections to a one-group cross section provides a representation of the environment within the subject TE. Also, the infinite-dilute data of the ORIGEN 238-group library does not automatically account for the shielding effects of the tallied TE. To generate results with the one-group approach of ORIGEN that are consistent with the continuous-energy approach of MCNP6, the self-shielded, one-group macroscopic cross sections for neutron absorption (Σ_a) in the various La and Te isotopes are derived using Eq. (1) and substituted for those automatically calculated by ORIGEN.

Each element in the La_3Te_4 material is specified at its naturally occurring isotopic composition and in proportion to a La_3Te_4 molecular compound [Figure 7].

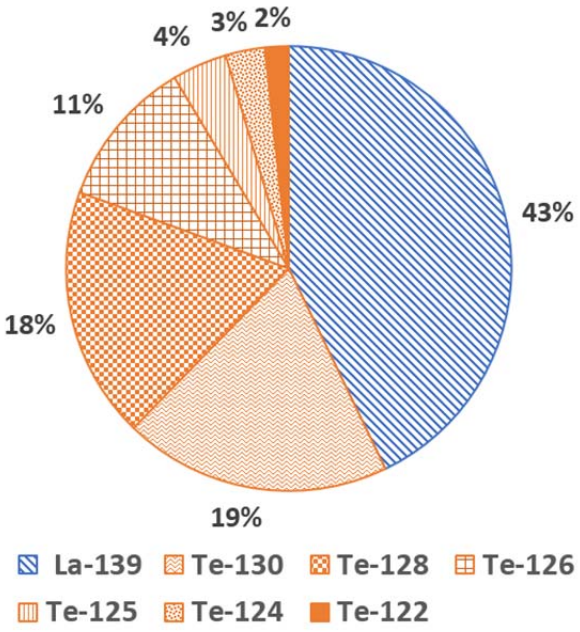

Figure 7. Isotopic compositions for La_3Te_4 TE components in simulation

The isotopic distribution is important to consider since each individual isotope presents a unique channel for transmutation when exposed to neutron fields. The element La is modeled as 100% ^{139}La, which presents a reaction channel that can produce ^{140}Ce, as shown in the neutron absorption (1), transmutation to ^{140}La (2), and β-decay to ^{140}Ce in Figure 8.

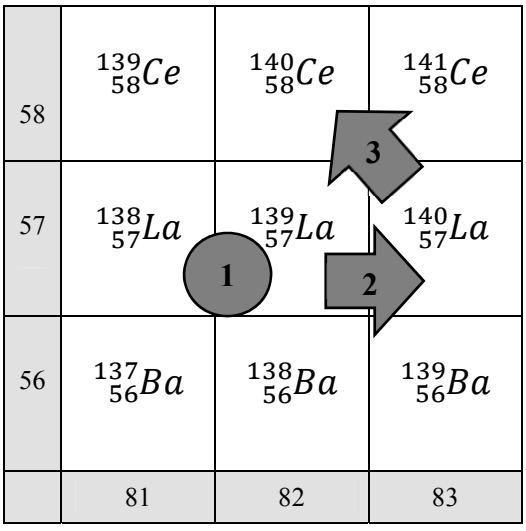

Figure 8. Example of ^{139}La Neutron Absorption (1), Transmutation to ^{140}La (2), and Subsequent β-Decay to ^{140}Ce (3).

While this is the most predominant transmutation channel for ^{139}La, there are other nuclear reaction potentials such as (n,t), (n,α), and (n,2n) that create trace amounts of Ba, Cs, and to a much lesser degree, Pr.

The top six most abundant naturally occurring Te isotopes all have their own unique neutron absorptions, decays, and transmutation probabilities that present a host of decay/production channels for various daughter isotopes. These reaction processes are too numerous and circuitous to effectively represent graphically. Table 2 shows the various target isotopes, the most probable reactions, and the final products from the top six Te isotope transmutation channels.

Table 2. Various Transmutation Channels for Te Isotopes.

Target Te Isotope	Significant Initial Reaction Types	Final Transmutation Products
^{130}Te	(n,γ), (n,2n), (n,p)	^{131}Xe, ^{129}I, ^{130}Sb
^{128}Te	(n,γ), (n,2n)	^{129}I, ^{127}I
^{126}Te	(n,γ), (n,2n)	^{127}I, ^{125}Te
^{125}Te	(n,γ)	^{126}Te
^{124}Te	(n,γ)	^{125}Te
^{122}Te	(n,γ)	^{123}Te

The solutions of these ORIGEN calculations can be output in a number of representations such as time-dependent mass, energy, or activity, and the elemental production/decay contributions can be broken down into contributions from individual isotopes. These data can be used in external post-processing programs or analyzed directly in a SCALE graphical user interface (GUI) known as Fulcrum [15].

5. PARTICLE TRANSPORT AND TRANSMUTATION RESULTS

The simulations for this analysis calculated the elemental and isotopic concentrations of La_3Te_4 TE materials at 1-year time steps over 20 years. The tabulated time-dependent mass concentrations of the top six most abundant transmuted elements are provided in Table 3, and the 20-year timesteps are shaded to highlight the maximum concentration values obtained.

Table 3. Time-Dependent Elemental Mass-Concentrations of Transmuted Materials in La_3Te_4 TE Modules Irradiated for 20-years by 18 GPHS Modules (in Grams)

yr	I	Ce	Xe	Sb	Sn	Ba
0	0.0E+00	0.0E+00	0.0E+00	0.0E+00	0.0E+00	0.0E+00
1	3.4E-15	1.6E-15	4.9E-16	2.7E-18	5.0E-19	1.4E-19
2	6.9E-15	3.1E-15	9.9E-16	6.2E-18	1.0E-18	2.8E-19
3	1.0E-14	4.7E-15	1.5E-15	9.6E-18	1.5E-18	4.2E-19
4	1.4E-14	6.3E-15	2.0E-15	1.3E-17	2.0E-18	5.6E-19
5	1.7E-14	7.8E-15	2.5E-15	1.6E-17	2.5E-18	7.0E-19
6	2.1E-14	9.3E-15	3.0E-15	2.0E-17	2.9E-18	8.3E-19
7	2.4E-14	1.1E-14	3.5E-15	2.3E-17	3.4E-18	9.7E-19
8	2.8E-14	1.2E-14	3.9E-15	2.6E-17	3.9E-18	1.1E-18
9	3.1E-14	1.4E-14	4.4E-15	2.9E-17	4.3E-18	1.2E-18
10	3.4E-14	1.5E-14	4.9E-15	3.2E-17	4.8E-18	1.4E-18
11	3.8E-14	1.7E-14	5.4E-15	3.5E-17	5.3E-18	1.5E-18
12	4.1E-14	1.8E-14	5.8E-15	3.8E-17	5.7E-18	1.6E-18
13	4.4E-14	2.0E-14	6.3E-15	4.1E-17	6.2E-18	1.8E-18

14	4.7E-14	2.1E-14	6.8E-15	4.4E-17	6.6E-18	1.9E-18
15	5.0E-14	2.3E-14	7.2E-15	4.7E-17	7.1E-18	2.0E-18
16	5.4E-14	2.4E-14	7.7E-15	5.0E-17	7.5E-18	2.1E-18
17	5.7E-14	2.5E-14	8.1E-15	5.3E-17	7.9E-18	2.3E-18
18	6.0E-14	2.7E-14	8.6E-15	5.6E-17	8.4E-18	2.4E-18
19	6.3E-14	2.8E-14	9.0E-15	5.9E-17	8.8E-18	2.5E-18
20¥	6.6E-14	3.0E-14	9.5E-15	6.2E-17	9.2E-18	2.6E-18

¥Bottom shaded row highlights the 20-year maxima.

Specific Isotopic Production

Any material consisting of different isotopes will produce different secondary isotope chains as a product of neutron irradiation. While Table 3 shows the top six elemental productions, the top six most prominent isotopes produced from La and Te transmutations are shown in Table 4.

Table 4. Time-Dependent Isotopic Mass Concentrations of Transmuted Materials in La_3Te_4 TE Modules Irradiated for 20 Years by 18 GPHS Modules (in Grams)

yr	^{127}I	^{129}I	^{131}I	^{131}Xe	^{131}Xe*	^{140}Ce
0	0.0E+00	0.0E+00	0.0E+00	0.0E+00	0.0E+00	0.0E+00
1	2.4E-15	9.4E-16	1.6E-17	4.9E-16	2.6E-19	1.6E-15
2	5.0E-15	1.9E-15	1.6E-17	9.9E-16	2.6E-19	3.1E-15
3	7.5E-15	2.8E-15	1.6E-17	1.5E-15	2.5E-19	4.7E-15
4	1.0E-14	3.8E-15	1.6E-17	2.0E-15	2.5E-19	6.3E-15
5	1.3E-14	4.7E-15	1.6E-17	2.5E-15	2.5E-19	7.8E-15
6	1.5E-14	5.6E-15	1.6E-17	3.0E-15	2.5E-19	9.3E-15
7	1.8E-14	6.6E-15	1.5E-17	3.5E-15	2.5E-19	1.1E-14
8	2.0E-14	7.5E-15	1.5E-17	3.9E-15	2.5E-19	1.2E-14
9	2.2E-14	8.4E-15	1.5E-17	4.4E-15	2.4E-19	1.4E-14
10	2.5E-14	9.3E-15	1.5E-17	4.9E-15	2.4E-19	1.5E-14
11	2.7E-14	1.0E-14	1.5E-17	5.4E-15	2.4E-19	1.7E-14
12	3.0E-14	1.1E-14	1.5E-17	5.8E-15	2.4E-19	1.8E-14
13	3.2E-14	1.2E-14	1.5E-17	6.3E-15	2.4E-19	2.0E-14
14	3.4E-14	1.3E-14	1.5E-17	6.8E-15	2.3E-19	2.1E-14
15	3.7E-14	1.4E-14	1.5E-17	7.2E-15	2.3E-19	2.3E-14
16	3.9E-14	1.5E-14	1.4E-17	7.7E-15	2.3E-19	2.4E-14
17	4.1E-14	1.5E-14	1.4E-17	8.1E-15	2.3E-19	2.5E-14
18	4.4E-14	1.6E-14	1.4E-17	8.6E-15	2.3E-19	2.7E-14
19	4.6E-14	1.7E-14	1.4E-17	9.0E-15	2.3E-19	2.8E-14
20¥	4.8E-14	1.8E-14	1.4E-17	9.5E-15	2.2E-19	3.0E-14

¥Bottom shaded row highlights the 20-year maxima
*Represents a metastable-state for ^{131}Xe

Choosing to focus on the highest concentration of transmuted elements and isotopes, the final (20-year), most abundant amounts of transmuted materials are shown in Figure 9.

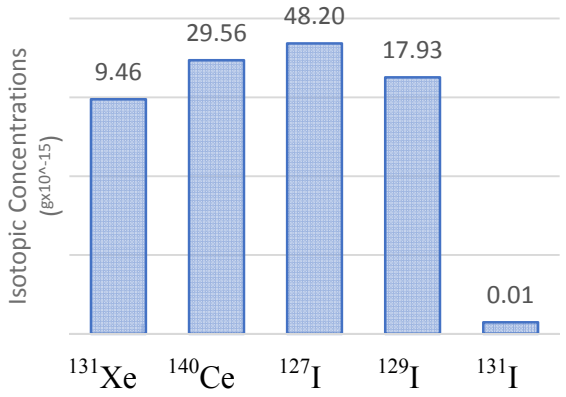

Figure 9. Mass concentrations of any isotope with a 20-year accumulation greater than 0.01 femtograms (1 fg = 1E-15 g).

6. CHEMICAL CONSIDERATIONS

The presence of unanticipated elements/isotopes in a thermoelectric module could have certain adverse effects on performance. This makes it important to evaluate the chemical impact of the transmutation events on an RTG. Data from Table 3 indicate that I, Xe, and Ce will be produced in a La_3Te_4 couple in the largest quantities, suggesting that these elements should be the initial focus of our analysis.

Because Xe is a noble gas, its chemical reactivity is essentially negligible. The production of a gas, however, could be concerning for an RTG that is sealed, as additional gases could cause pressurization and changes in the thermal conductivity of a generator. Results for the production of Xe from an ARTG, with 572 couples containing La_3Te_4 segments, indicate that after 20 years, the transmutation events will only produce 4.1×10^{-14} moles of Xe. Using the ideal gas law, the degree of pressurization created by the production of Xe can be estimated. Assuming that the RTG has an open volume of 20 L and an average gas phase temperature of 500 °C, the pressure of Xe is only 1.3×10^{-13} bar. This number is so small that it will not have any impact on the pressure or thermal conductivity of the generator, even under the most extreme but still rational conditions. Therefore, it can be concluded that the production of Xe resulting from transmutation events is not a concern for a theoretical ARTG design.

Iodine production in an RTG is far more interesting from a chemical perspective. Iodine compounds tend to be highly volatile and decompose at the proposed operational temperature for a La_3Te_4 segment (i.e., ~1,000 °C). In addition, at these high temperatures and under extremely low iodine partial pressures, the most favorable form of iodine is the monatomic gas. This is particularly interesting because under standard temperature and pressure (STP)

conditions, iodine tends to take on its molecular form, I_2. The fact that the monatomic form is preferable is interesting for several reasons.

First, it suggests that iodine will readily convert from an ionized state back into its monatomic ground state. When iodine is initially created in the Le_3Te_4 matrix, it will be due to the transmutation of Te. As such, the iodine will take on some of the anionic character of the Te atom in the La_3Te_4 matrix, suggesting that the iodine will start in the matrix as I^-. As an ion, I^- is not likely to be highly mobile, and the electrostatic forces in the La_3Te_4 matrix will help keep the I^- bound up within the TE material. The fact that monatomic iodine is stable under RTG-like conditions suggests that iodine will more readily give up its ionic character. As a neutral atom, the mobility of iodine through the TE matrix, or along grain boundaries within the TE material is likely to increase dramatically. With all of these factors combined, iodine is likely to evolve from the La_3Te_4 matrix and find its way to the gas phase of the RTG.

Second, as a monatomic species, iodine is a free radical. Free radicals are notoriously reactive, indicating that gaseous iodine would readily react with a number of different materials within an RTG, including the metallization and bonding layers in the TE couples.

Fortunately, the amount of total iodine produced via transmutation is still very small. After 20 years, only 66.1×10^{-15} g of iodine have been produced. This quantity is not large enough to impact any surrounding materials via a direct chemical reaction mechanism. As an experiment, the total iodine production predicted from a single couple was allowed to react with a hypothetical 20 μm thick bonding wafer of Ti which was ostensibly used to bond the various segments of the TE couple together using FactSage thermochemical software [16]. Iodine can react with Ti to form TiI, TiI_2, and TiI_3, all of which are volatile at the proposed La_3Te_4 operational temperatures. In the worst-case scenario, the iodine would attack the edges of the Ti wafer to form TiI. In this case, the amount of iodine present would react with 0.14 pm of the Ti wafer. This number is irrationally small by several orders of magnitude (the atomic radius of Ti = 215 pm), indicating that a direct chemical reaction with the Ti bonding wafer is not a concern. Using a hypothetical Ti bonding wafer is a good worst-case example, as it represents a critical component in the RTG system that is also one of the smallest individual components.

In a similar experiment, the complete quantity of iodine was allowed to dissolve into the matrix of the Ti bonding wafer. This resulted in an iodine impurity of 0.11 ppb within the Ti wafer. Again, this number is small enough that the properties of the bonding wafer are not expected to change.

One might also consider the implications of the total iodine production from all 572 couples that could be present in a theoretical ARTG [2], but even in this case, the quantity of iodine is too small to be a concern. As a first-order estimate, if it is assumed that all 572 couples produced 66.1×10^{-15} g of iodine over 20 years, that is still only enough to react with a single Ti wafer to a depth of 80 pm or to dissolve in a single Ti wafer to an impurity concentration of 63 ppb. Even without the difficulty of all the iodine getting to a single wafer in a single couple, along with other assumptions that make this first-order estimate conservative,[1] this number is still irrationally small.

Based on this analysis, it can be concluded that the production of iodine due to the transmutation events predicted in this study does not pose any risk to an RTG from direct chemical reaction.

However, in addition to direct chemical reaction, iodine creates the possibility of a cyclic chemical reaction that could pose a risk to an RTG system. Figure 10 presents an example of a cyclic reaction that could occur between iodine and titanium within an RTG. In this example, iodine reacts with the surface of the Ti to form TiI_2, which is a gas at the proposed La_3Te_4 operational temperatures. This gas then migrates to a cooler portion of the RTG and deposits the TiI_2 as a solid. Even at cooler temperatures ranging all the way down to ~200 °C, iodine can still form the monatomic gas. This means that the iodine can dissociate from the TiI_2, leaving behind a deposit of Ti. The monatomic iodine gas could then return to the source of Ti to react again. While this example specifically cites Ti, the same cyclic reaction could occur with a very large variety of other elements because almost all iodides are volatile at RTG temperatures, so most elements will react in the same manner as Ti.

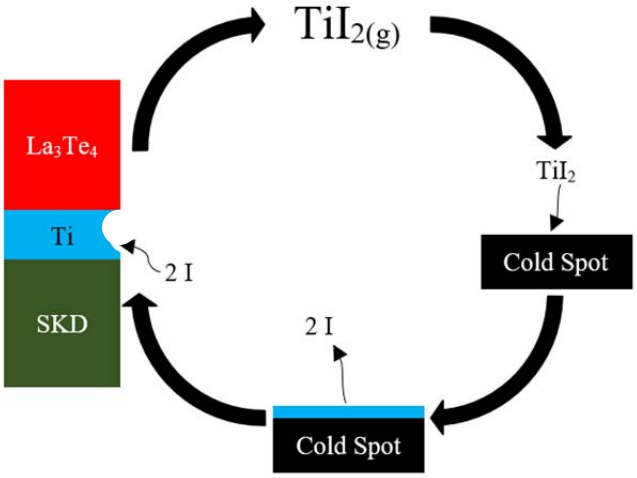

Figure 10. Example Cyclic Reaction between Titanium and Monatomic Iodine That Could Cause Erosion in Critical Components in an RTG

While this cyclic reaction could be highly detrimental to a large number of RTG components, the risk of this cyclic reaction is considered very low. Even in a theoretical RTG

[1] For example, TE couples that are not positioned directly over the centerline of the fuel stack will have fewer transmutation events.

that possessed 572 couples in operation for 20 years, the maximum iodine pressure that could be present is only estimated to be ~10^{-12} bar. Chemical reaction rates are almost always proportional to the partial pressure of the reactant, in this case iodine, and this is an extremely small pressure. Therefore, even if a cyclic reaction is possible, the rate is likely to be very slow. As a result, the risk of a cyclic reaction between iodine and other RTG components is estimated to be extremely low.

The risk posed by this cyclic chemical reaction is reduced even further if the ARTG design is vented to the vacuum of space as is done in the heritage GPHS-RTGs. In this instance, the build-up of iodine would be decreased because the iodine would have a pathway to leave the RTG. The predicted partial pressure of iodine is on the same scale as the vacuum of space, indicating that there may not be any major driving forces to extract the iodine from the generator. Despite the lack of a driving force, over the course of 20 years, it is very likely that most of the iodine would find a diffusive pathway out of the generator. Therefore, in an RTG design that is open to space, the production of iodine poses no risk to the RTG.

Finally, the total production of cerium is approximately 45% of the total iodine production. From all 572 couples in a theoretical ARTG, this equates to ~29.5×10^{-15} g of cerium over 20 years. As with iodine, this analysis has led to the conclusion that the production of cerium due to transmutation events as predicted in this study does not pose any risk to an RTG due to direct chemical reaction.

For completeness, a first-order evaluation was conducted to resolve the potential effect of produced cerium in a La_3Te_4 segment and several potential metallization materials at an operational temperature of ~1,000 °C. Within the La_3Te_4 segment, cerium could form a solid solution with lanthanum where one chemical species is substituted for another. This result is corroborated by anecdotal evidence that was obtained when La_3Te_4 materials were doped with Ce. In these doped materials, the Ce readily substituted onto the La site with minimal change in the properties of the La_3Te_4 base material [17]. However, cerium will also form six different intermetallic compounds with tellurium, suggesting that if the concentration of cerium became large enough (which is not the case here), other cerium tellurides could begin to form within the material. Considering potential metallization materials, cerium would form a solid solution with niobium, titanium, and zirconium, and it would form intermetallic compounds with iron, nickel, and tungsten. Interestingly, the melting point of the intermetallic compounds of cerium-iron and cerium-nickel are below 1000 °C. Although intriguing, a detailed thermodynamic analysis would be required to predict the behavior of the cerium produced in the TE element or any metallization layer. In this case, however, the quantity of cerium is too small to be of concern, so a more thorough analysis is not warranted.

The analysis presented in this paper is predicated on two major inputs. The first input is that the GPHS fuel stack is the source of the radiation field. Changing the size of the GPHS fuel stack will not produce a large enough change to the radiation field to cause a major change to the results presented here. Thus, it can be said that these results should hold true for any GPHS-based RTG. If the materials are exposed to higher neutron radiation fields such as those created by an actual nuclear reactor, then it is possible that the quantities of transmuted elements will become significant. In such a case, it is recommended that the analysis performed in this study be repeated with the neutron fluence levels predicted in a reactor scenario.

The second major input is the quantity of TE material present in the system. In the ARTG design, the quantity of La3Te4 is small compared to the mass and volume of other parts of the RTG. If the quantity of La3Te4 is increased by a few orders of magnitude, then the quantities of transmutation products might become a concern. The same can be said of other materials in the RTG design. If the quantity of those materials is orders of magnitude larger than the TE materials, then it is possible that the transmutation products from those materials could pose a risk to the RTG. In that case, the analysis described herein should be performed on the other material.

7. CONCLUSIONS

This analysis demonstrated that despite the low neutron flux levels present in an RPS setting, the production of non-TE materials through neutron transmutation is possible in TE modules used in RPS over a notional 20-year mission. It was demonstrated that nuclear transport and transmutation software such as MCNP6 and ORIGEN can be coupled with FactSage to perform high-resolution calculation methods to determine the neutron activation/transmutation effects and resulting chemical reaction potentials that are likely to be observed during a notional 20-year mission for ARTG designs. While this was a specific investigation of ARTG designs, this methodology can be employed for any material being proposed for TE modules, RPS design, and other non-TE RPS materials.

For the hypothetical RTG analyzed, the mass concentrations of transmuted elements and isotopes in the La_3Te_4 thermoelectric segments do not pose any risk due to direct chemical reaction. Thus, the generation of neutrons from spontaneous fission and alpha-neutron (α,n) reactions from the decay of $^{238}PuO_2$ does not contribute to any potential transmutation or chemical performance degradation mechanisms for this system. A cyclic chemical reaction involving transmuted iodine is suspected for an ARTG design that includes La_3Te_4 segments but given the extremely small quantities of iodine produced over a notional 20-year mission, the risk of this cyclic chemical reaction is estimated to be very low to nonexistent for any ARTG design. However, it would be prudent to conduct similar first-order analyses on other future RPS and/or

hybrid fission-TE system designs to accurately predict lifetime performance of the systems and to retire any concerns associated with potential risks from transmutation of TE or non-TE materials used in nuclear space power systems.

ACKNOWLEDGMENTS

Portions of this effort were funded under Battelle Energy Alliance contract 00184172 to the University of Dayton. The authors would like to thank June Zakrajsek of the National Aeronautics and Space Administration (NASA) RPS Program office and Dr. Stephen Johnson of the Idaho National Laboratory (INL).

REFERENCES

[1] Y. Lee and B. Bairstow, "Radioisotope Power Systems Reference Book for Mission Designers and Planners," Jet Propulsion Laboratory (JPL), JPL-Publication 15–6, 2015.

[2] W. Otting, "Advanced Radioisotope Thermoelectric Generator (ARTG) Leverages Segmented Thermoelectric Technology," presented at the Nuclear and Emerging Technologies for Space 2015, Albequerque, NM, 2015.

[3] B. Bairstow and Y. Lee, "Radioisotope Power Systems Reference Book for Mission Designers and Planners," 2015.

[4] G. J. Snyder and T. S. Ursell, "Thermoelectric Efficiency and Compatibility," *Phys. Rev. Lett.*, vol. 91, no. 14, Oct. 2003.

[5] T. G. George and D. Pavone, *General-purpose heat source safety verification test series: SVT-11 through SVT-13*. Los Alamos National Laboratory, 1986.

[6] G. L. Bennet *et al.*, "The Mission of Daring: The General-Purpose Heat Source Radioisotope Thermoelectric Generator," presented at the 4th International Energy Convention Engineering Conference and Exhibit, 2006.

[7] R. L. Cataldo and G. L. Bennett, "US Space Radioisotope Power Systems and Applications: Past, Present and Future," NASA Jet Propulsion Laboratory (JPL), JPL Publication 15–6, 2011.

[8] K. S. Krane and D. Halliday, *Introductory nuclear physics*. New York: Wiley, 1987.

[9] G. M. Matlack and C. F. Metz, "Radiation Characteristics of Plutonium-238," Los Alamos National Laboratory, Los Alamos, NM, LA-3696, 1967.

[10] G. H. Rinehart, "Design characteristics and fabrication of radioisotope heat sources for space missions," *Prog. Nucl. Energy*, vol. 39, no. 3–4, pp. 305–319, 2001.

[11] "National Nuclear Data Center, information extracted from the Chart of Nuclides database." [Online]. Available: http://www.nndc.bnl.gov/chart/. [Accessed: 01-Jan-2016].

[12] T. Goorley *et al.*, "Features of MCNP6," *Ann. Nucl. Energy*, vol. 87, pp. 772–783, 2016.

[13] B. Rearden and M. Jessee, "SCALE Code System," Oak Ridge National Laboratory (ORNL), Technical Report ORNL/TM-2005/39, Aug. 2016.

[14] H. Bateman, "Solution of a System of Differential Equations Occurring in the Theory of Radioactive Transformations," *Proc. Camb. Philos. Soc. Math. Phys. Sci.*, vol. 15, 1910.

[15] R. Lefebrve, "Fulcrum User Interface," Oak Ridge National Laboratory (ORNL).

[16] C. W. Bale *et al.*, "FactSage thermochemical software and databases," *Calphad*, vol. 26, no. 2, pp. 189–228, 2002.

[17] S. K. Bux, "Discussion with Sabah Bux," 27-Sep-2018.

BIOGRAPHY

Michael B. R. Smith *received a BS in Nuclear Engineering with a concentration in Radiological Nuclear Engineering from The University of Tennessee in 2016 and an MS in Nuclear Engineering in 2017. He has been involved in internships and research projects throughout this time covering topics such as nuclear thermal propulsion (NTP), galactic cosmic ray transport, radioisotope power sources (RPSs), and prompt neutron background signals at the Spallation Neutron Source. He currently works as a research scientist at Oak Ridge National Laboratory for the Advanced Reactor Engineering Group. He currently serves on multiple NASA-funded projects involving RPS and NTP technologies, including dynamic RPS technology assessments, software development for radiation concerns from RPSs, and transient modeling for NTP.*

Christofer E. "Red Shirt" Whiting *received his BS in Chemistry from the University of Minnesota in 1999 and a PhD in Analytical Chemistry in 2007. For the past 7 years he has worked as a research scientist at the University of Dayton Research Institute, where he supports the US Department of Energy's Space and Defense Power Systems Program. Chris's research specializes in the solid-state chemistry of the* $^{238}PuO_2$ *fuel used in radioisotope thermoelectric generators through surrogate and direct experimentation. He also supports development of the enhanced Multi-Mission Radioisotope Thermoelectric Generator, a next-generation power system for use in various space exploration missions.*

Chadwick Barklay *is responsible for leading the Advanced High-Temperature Materials Group at the University of Dayton Research Institute (UDRI), which is composed of scientists, engineers, and technicians who conduct cutting edge sponsored material-based research and development for various sponsors including the US Department of Energy (DOE), NASA, the US Department of Defense (DoD), and a wide range of industrial partners. He has 26 years of experience in the assembly, testing, and transportation of RPS units, and he has participated in a number of formal programmatic review committees for DOE and NASA on a broad range of technical areas.*